Journal of Positive School Psychology
2023, Vol. 7, Issue 2
Pp 89-103

Spatiotemporal dynamics of agricultural drought and food insecurity in Asia

Riaz-ul-Hissan
Department of Geography, Government Graduate College Gojra, Pakistan.
Liaqat Ali Waseem
Department of Geography, GC University Faisalabad, Pakistan
Hamza Shafiq
Department of Geography, Government Graduate College Gojra, Pakistan.
Muhammad Shahid Maqbool
Department of Economics, Government Graduate College Gojra, Pakistan.
Muhammad Waqee Ur Rehaman
Department of Physics, Government Graduate College Gojra, Pakistan.
Muhammad Ahmad
Department of Economics, Government Graduate College Gojra, Pakistan.
Arjumand Zahra
Department of Geography, Government Graduate Viqar un Nisa College Rawalpindi, Pakistan.

Abstract
The current study deals with the drastic effects of agricultural drought which is the slowest among all the natural hazards and turns the green vegetated lands into barren lands. Several indices have been developed so far to monitor the drought and drought conditions. In this present research, the analysis of remote sensing data for the agricultural drought acquired from the United State Geological Survey is reported. The satellite imagery of Landsat 7 and Landsat 8 for the years 2011-2022 were obtained and Normalized Difference Vegetation Index (NDVI), Vegetation Condition Index (VCI), Land Surface Temperature (LST), Temperature Condition Index (TCI) and Vegetation Health Index (VHI) were employed to examine the empirical analysis. The study area was classified into five categories based upon the severity of agricultural drought in percentage. The results reveal a substantial increase in drought area from 2011 to 2022. In 2011, it was observed that the extreme drought area was 2.0081% of land which increased to 8.452% in 2022. The findings of OLS method illustrate that severe drought and extreme drought had a significant negative impact on agriculture value added share of GDP during the reported time. Moreover, the extreme drought had a significant positive impact on food insecurity during the selected time span. This study will be highly beneficial for the policy makers and organizations involving in the protection of the green land from drought.

Keywords: Agricultural Drought, Food insecurity, Vegetation Health Index, Remote Sensing, Extreme Drought

Article History:
Received: 20th May, 2023
Accepted: 19th Jun, 2023
Published: 23rd June, 2023

1. Introduction:

Drought is a very harsh and frequent occurring hydro- meteorological natural hazard that adversely affected human, animal and vegetation\(Liu, Zhu, Pan, Bai, & Li, 2018; Mullapudi, Vibhute, Mali, & Patil, 2023). Revealed in their research study that climatic conditions have changed the (Mullapudi et al., 2023)rainfall pattern and its distribution accompanied by tremendous increase in temperature across the globe which ultimately gave birth to repeated and frequent droughts There exists a remarkably close relationship among metrological droughts, agricultural droughts, and anthropogenic activities. So, in this regard, monitoring of both droughts, metrological and agricultural, is dire need of the hour. Due to the explosive growth of population, it is hard to gather real-time ground observations and keep track of the vegetation needed for agricultural droughts. During the past few year's agricultural production has shown sharp decline along with a severe damage to the natural ecosystems and habitat due the increasing droughts and drought conditions prevailing all over the world(Sevanto, 2018). Drought is considered to be the most expensive

natural disaster as it casts significant impact causing both, damage and loss, to a large number of populations across the world(Lott & Ross, 2006; Tadesse, Brown, & Hayes, 2005). so in this regard, the dire need of the hour is to develop a sound and authentic monitoring technology and system(Otkin, Anderson, Hain, & Svoboda, 2014). Drought might be of varying natures and intensities. The intensity of the drought is determined by the difference in the precipitation of a particular place for a specific period as compared to the total amount of the precipitation received by that region or area during the same period. However here lies a difficulty to observe the beginning and ending as well as the characteristics such as geographical boundary, duration, and intensity of the drought as it is considered a "creeping disaster"(Bajgain et al., 2017; Bajgain, Xiao, Wagle, Basara, & Zhou, 2015; Vicente-Serrano, Beguería, & López-Moreno, 2010; Zhou et al., 2017). So, while doing evaluation of the droughts and their conditions, their mode of occurrence and distribution with reference to time and place must be identified first(Nam, Choi, Yoo, & Engel, 2012; Nam, Hayes, Svoboda, Tadesse, & Wilhite, 2015). After the identification, the second most thing is to quantify the impact and effects of the areas which are affected by the drought(Nam et al., 2018; Svoboda, 2000; Wilhite & Glantz, 1985).

Drought is one of the most complicated and complex natural disasters. Main characteristic of the drought is its slowness in origin, evaluation and spreading over a very vast area(Andersson et al., 2020; Dikshit, Pradhan, & Huete, 2021; West, Quinn, & Horswell, 2019; Zhong, Di, Sun, Xu, & Guo, 2019). The natural mechanism that controls and assesses the duration, intensity and spatial extent is also complex in nature as well and is not easily perceptible. The drought cast a significant impact on the local population and all the agro-based activities and ecosystems. According to the Unites Nations for Disasters Risk reduction (UNDRR) 61.7 were affected directly or indirectly by natural disasters causing a death toll of 4733. The Intergovernmental panel on climate change (IPCC) revealed the facts in its recently published report 2022 that in the next 30 years about 2.5 million people in the developing countries will be more affected by the droughts.

The agricultural drought that is developed, flourished and spread by inter seasonal phenomenon across the globe having characteristic and defined as very low level of soil moisture which encompasses a large number of variables(Chandrasekara, Kwon, Vithanage, Obeysekera, & Kim, 2021; Chen, Zhong, Pan, Xie, & Kim, 2020; Das, Noguchi, & Ahamed, 2021; Y. Gao, Gao, Damdinsuren, & Dorjsuren, 2021; Jiménez-Donaire, Giráldez, & Vanwalleghem, 2020; Wildemeersch, Garba, Sabiou, Fatondji, & Cornelis, 2015). That is why the prediction and perception of the drought correctly is immensely difficult(Ghazaryan, Dubovyk, Graw, Kussul, & Schellberg, 2020; Hara, Piekutowska, & Niedbała, 2021). Agricultural drought is more sensitive to the climatic variables than the other all natural disasters. Beside climatic variables, other geographical, agronomic, soil and anthropogenic factors also play a vital role in creation and spared of agricultural drought(Araneda-Cabrera, Bermúdez, & Puertas, 2021; Bayissa, Tadesse, & Demisse, 2019; Bento, Gouveia, DaCamara, Libonati, & Trigo, 2020; Bezdan et al., 2019; Das et al., 2021; Ghazaryan et al., 2020; Han, Bai, Yan, Yang, & Ma, 2021; Kulkarni et al., 2020; Yang et al., 2016). reveal that there has been an increase of about 12.7% in the drought globally in the past recent years.

The study of droughts not only aims at just identifying drought conditions and gathering data but also includes the various indices to monitor as well. On a world level, if all the known approaches agglomerated together, there are 150 main indices used to assess the drought classification and monitoring(Finnessey, Hayes, Lukas, & Svoboda, 2016). Most of these indices are developed for specific geographical locations and climatic conditions(Hanade Houmma, El Mansouri, Gadal, Mamane Barkawi, & Hadria, 2022; Liu et al., 2018; Liu et al., 2020; Mishra & Singh, 2010; Naumann et al., 2014; Song, Wang, Ge, & Xu, 2020; Zhang, Jiao, Zhang, Huang, & Tong, 2017).

There are various indices used frequently to analyze the distribution and occurrence of the droughts Standardized Precipitation Index (SPI), Palmer Drought Severity Index (PDSI) or Standardized Ground water level Index (SGI) for spatial distribution all the related indices are interpolated by applying stations' point data which are later mapped for display. For inaccessible areas and for larger spatial area satellite imagery is used(Clark & Roberts, 2012; Groten, 1993; Quarmby, Milnes, Hindle, & Silleos, 1993). There are numerous studies which are using satellite imagery for drought monitoring. There are many indices based on satellite imagery used to monitor the droughts such as The Leaf Area Index (LAI), Normalized difference vegetation index (NDVI) the Enhanced Vegetation index (EVI). All these indices are interred, linked, and connected in one way or the other. Some of these are used to evaluate the various biological characteristics of the vegetation while others are important to chemical and thermal characteristics(Berger, Ettlin, Quincke, & Rodríguez-Bocca,

2019; Clark & Roberts, 2012; Fang, Liang, & Hoogenboom, 2011; B.-C. Gao & Li, 2000; F. N. Kogan, 1995). such as Vegetation Health Index is used to determine the drought severity, detection, and duration(Seiler, Kogan, & Sullivan, 1998). In this this study main indices used include Normalized Difference Vegetation Index, Vegetation Condition Index, LST, TCI and VHI.

2. Material and Method

Study Area

The Pacific Ocean is in the east of Asia almost surrounded by the water bodies from all sides. The Ural Mountains and the Mediterranean Sea is in the west, In north, the Arctic Ocean and the Indian Ocean in the south. Similarly, Greater Asia is spreading vastly, from 80 degrees north latitude to 8 degrees south latitude and between 30 degrees east longitude and 170 degrees east longitude(Wang, 2004).

Due to its huge area and versatility in nature, Asia has dynamic climatic conditions and regions. There are seven types of climatic regions in the Asia which are Equatorial region, Monsoon region, Central Asian desert region, Temperate grasslands, Cold temperate region, Roman Region, and Tundra region. Asia has deserts like the Gobi Desert, Thar Desert, Karakum Desert, Thal Desert, Rajhistan Desert, Cholistan Desert, Negev Desert, Ryn Desert, and Aralkum Desert(Putnam et al., 2016).

South-West Asia and Central Asia get the minimum rainfall, and it is 50 cm per year. On the hand, South-East Asia and southern and Central China receive the normal rainfall that is 100 cm to 200 cm per year. The northern part of the India also gets the normal rainfall. The equatorial region of Asia receives the maximum rainfall, and it is more than 200 cm per year. So, South-west Asia has more chance of drought conditions because of low precipitation rate and higher evaporation rate. The soil moisture of that region will decrease and vice versa. The drought conditions are also accelerated by the changing climate and severity of the seasonal spells(X. Gao, Xu, Zhao, Pal, & Giorgi, 2006).

Fig. 2 shows the study area.

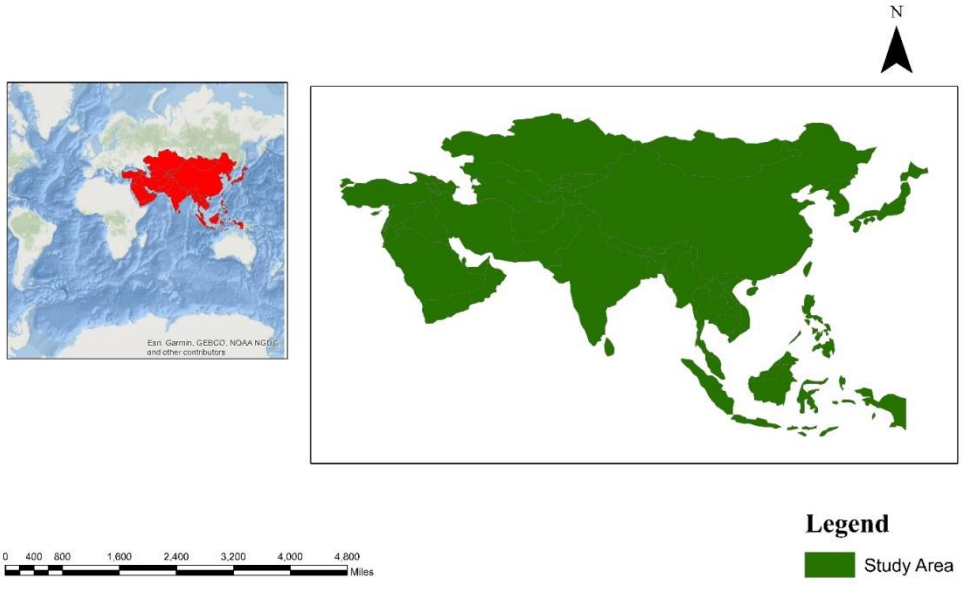

Data Source

Remote sensing data for the agricultural drought of study area was acquired from the Earth Explorer (USGS) https://earthexplorer.usgs.gov/. The imagery of Landsat 7 and Landsat 8 were acquired for monitoring agricultural drought in the study area from 2011-2022. The Landsat 7 imagery has the scanline error which was

removed with the Landsat toolbox in the ARC GIS. The data was acquired on food insecurities from Food and Agriculture Organization of United Nations (FAO) from 2014-2022 https://www.fao.org/faostat/en/#data/FS and agricultural share of value addition to GDP from Food and Agriculture Organization of United Nations (FAO) from 2011-2022 https://www.fao.org/faostat/en/#data/SDGB.

3. Methodology

Monitoring of Agricultural Drought

Landsat 7 and 8 imageries from 2011-2022 were used to analyze agricultural drought. Multispectral data of Landsat 7 and 8 was used to calculate the Normalized Difference Vegetation Index of the interested area. To calculate the Land Surface Temperature of the study area thermal bands of the Landsat 7 and 8 were used.

NDVI Calculation

For the NDVI, the multispectral data of the Landsat 7 and 8 was used and it has bands difference to calculate the NDVI of the interested area. For the NDVI, the Landsat 7 imagery has band 4 as the NIR band while the Landsat 8 imagery has band 5 as the NIR band. There is also a difference in the red band for the Landsat 7 and Landsat 8. Band 3 represents the red band in the Landsat 7 imagery and band 4 represents the red band in the Landsat 8 imagery. The formula of the NDVI is presented in (Eq. 1).

$$NDVI = (NIR - RED\ Band) / (NIR + RED\ Band) \quad (1)$$

The values of the NDVI range lies between -1.0 as the low value and 1.0 as the high value. The dense vegetation always lies between the range 0.2 to 0.9 (Bustos & Meza, 2015), on the other hand, the values less than 0.1 represent the rocks, water bodies and open spaces (Fu & Burgher, 2015).

VCI (Vegetation Condition Index)

The vegetation condition index is based on NDVI that is used to calculate the vegetation condition in the study area and used for the assessment of the drought condition (Gebrehiwot, Van der Veen, & Maathuis, 2011). (Gebrehiwot, Van der Veen, & Maathuis, 2016) stated that vegetation condition index is more advisable to monitor agricultural drought and gives authentic information to assess momentary agricultural droughts during the crop growing season. As (F. N. Kogan, 1995) verified, vegetation condition index is calculated from the NDVI. The VCI data are constructed by (Eq 2).

$$VCI = 100 * ((NDVI\ a - NDVI\ min) / (NDVI\ max - NDVI\ min)) \quad (2)$$

Where,

The current value of NDVI is represent with NDVI a

The minimum NDVI values throughout the period is represent with NDVI min.

The maximum NDVI value throughout the period is represent with NDVI max.

(Fu & Burgher, 2015; Gebrehiwot et al., 2016; F. Kogan, 2002) reputed that the agricultural drought was classified into four classes on the bases of VCI (Table 1).

Table 1 Classes value of Vegetation Condition Index scheme for drought

Drought Condition	Value in Percentage
Extreme Drought	<10
Severe Drought	>35
Mild Drought	>50
No Drought	>100

The vegetation condition index is also known as the drought monitoring tool (Dutta, Kundu, Patel, Saha, & Siddiqui, 2015); Furthermore, vegetation condition index was quite enough to explain the authentic drought condition of the area or the region. So, temperature condition of the area or region plays a vital role in the drought condition assessment. For the improvement of temperature condition index, temperature condition was captured to differentiate the vegetation behavior of the area. Temperature condition Index can be calculated by the land surface temperature of the study area with the thermal data of Landsat 7 and 8 for the drought monitoring from 2011 to 2022.

Calculating of LST (Land Surface Temperature)

To calculate the LST, the thermal bands of Landsat 7 and Landsat 8 are used. So, the Land Surface Temperature was calculated from band 6 of the Landsat 7 and band 10 of the Landsat 8 (Guo, Ren, Zheng, Lu, & Dong, 2020).

The TOA radiance of thermal bands of Landsat 8 with TIR sensor retrieve from digital number (Alves, 2016). Consequently, Land Surface Temperature was calculated by using the BT of thermal infrared bands, mean and difference in LSE of the study area(Cheng, Nnadi, & Liou, 2015).

Conversion DN to TOA Spectral Radiance.

The data of thermal band of the Landsat sensor and it gives a values to pixels that are stored in the DN that is not calculated yet and converted into spectral radiance units (How Jin Aik, Ismail, & Muharam, 2020) by use (Eq 3).

$$L\lambda = (ML * Q\,Cal) + AL - 0.29 \quad (3)$$

Where:

Lλ= TOA radiance.

ML= 0.00038000

AL= 0.10000

Q Cal= Band 10 or Band 6

-0.29 = the inaccuracy of radiance

Conversion TOA to BT

After the conversion radiance from the digital number values, the spectral radiance of thermal bands should be calculated BT as shown in (Eq 4).

$$BT = (k2 / (\ln (K1 / L\lambda) + 1)) - 273.15 \quad (4)$$

BT= Brightness Temperature

K2 = 1329.205

K1 = 799.0284

Lλ = TOA

Ln: is natural logarithm.

And the value 273.15 is used to convert the temperature k0 to C0.

Calculate LSE using NDVI.

The NDVI was used to differentiate the distributions of vegetation covers. Furthermore, it is create the revision of NDVI into values correlated with vegetation cover portion (Tomar, Kumar, Rani, Gupta, & Singh, 2013). To calculate proportion of vegetation (PV), the NDVI is particularly important.

The NDVI is calculated from (Eq 5).

NDVI = (NIR – RED) / (NIR + RED) (5)

Where,

NDVI = Normalized Difference Vegetation Index

NIR = Near Infrared Band

RED = Red Band

Retrieval of PV

The PV (proportion of vegetation) is calculated by (Eq 6).

PV = Square ((NDVI-NDVI min) / (NDVI max – NDVI min)) (6)

Calculating LSE

Land surface emissivity (LSE) is particularly important to estimate Land Surface Temperature. According to (Sobrino, Jiménez-Muñoz, & Paolini, 2004), land Surface emissivity is calculated by (Eq 7).

E = 0.004 ∗ PV + 0.986 (7)

The calculated RST (Radiant Surface Temperature) were for emissivity using (Eq. 8)

LST = (BT / (1+ (λ* BT / P) *ln (E))) (8)

Where,

LST = Land Surface Temperature

BT = Brightness Temperature.

λ = 0.00115

$\rho = 1.4388$

E = Land Surface Emissivity.

The Temperature Condition Index was calculated by the (Eq. 9)

$$TCI = 100 * ((LST\ max - LST\ a) / (LST\ max - LST\ min)) \quad (9)$$

Where:

LST a = the value of current month LST,

LST min = the minimum value of the LST

LST max = the maximum value of the LST.

Finally, the Vegetation Health Index was calculated by TCI and VCI to assess both drought conditions. The VHI was calculated by (Eq 10).

$$VHI = (0.5 * VCI) + (0.5 * TCI) \quad (10)$$

Where:

VHI = Vegetation Health Index.

a = 0.5 (contribution of VCI and TCI).

VCI = Vegetation Condition Index.

TCI = Temperature Condition Index.

Vegetation Health Index was classified into five classes according to VHI and TCI Scheme (F. Kogan, 2002). These are the VHI classes for Agricultural Drought monitoring (Table 2).

Table 2 Classes value of Vegetation Health Index scheme for drought.

Agricultural Drought Class	Value in Percentage
Extreme Drought	<10
Severe Drought	20
Moderate Drought	30
Mild Drought	40
No Drought	>40

4. Results and Discussion

This study aims at finding out the agricultural drought and its conditions in Asia the drought conditions in Asia. The agricultural drought is investigated based on vegetation health index and retrieves the drought classes from it. The south-west Asia faces more drought conditions as compared to Central Asia. The equatorial region of Asia faces moderate and mild drought conditions.

Vegetation Health Index

Fig. 2 shows the intensity of drought conditions in the different area of Asia like southern, northern, south-west, south-east, and central Asian regions. In 2011, the extreme drought condition is 2.01%, severe drought condition is 3.96%, moderate drought condition is 12.47%, mild drought condition is 23.20%, and 58.4% had zero drought condition. In 2012, the extreme drought condition get height and become 3.11%, severe drought

condition is also increase and become 5.56%, moderate drought condition is increase and become 12.94%, mild drought condition decrease and become 20.34%, and the percentage of zero drought condition will decrease and become 58.05%. In 2013, the extreme drought again gets his height and become 4.22%, severe drought condition is decrease and become 4.15%, moderate drought condition is also decrease and become 11.18%, mild drought condition is decreased and become 19.97%, and the percentage of zero drought condition will increase and become 60.48%. In 2014, the extreme drought condition is decrease and become 4%, severe drought condition is also decrease and become 3.91%, moderate drought condition is again decrease and become 10.81%, mild drought condition is decreased and become 19.76%, and the percentage of zero drought condition will increase and become 61.53%.

Fig. 2 shows the drought condition variation 2011-2014

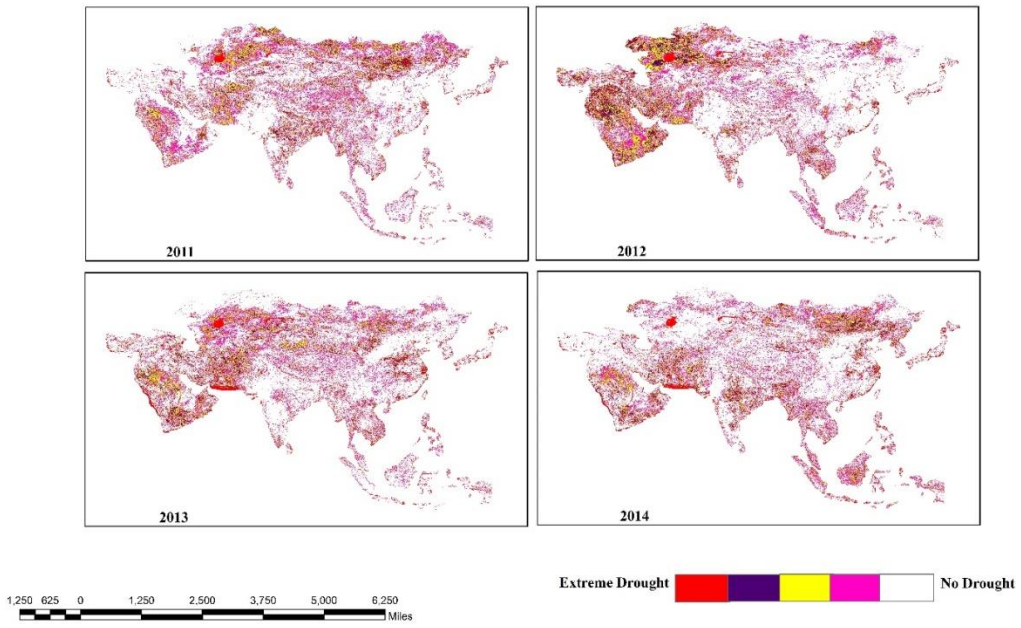

Fig. 3 shows the intensity of drought conditions in the different area of Asia like southern, northern, south-west, south-east, and central Asian regions. In 2015, the extreme drought condition is increased and become 4.89%, severe drought condition is also increase and become 4.95%, moderate drought condition is decrease and become 10.70%, mild drought condition is also decrease and become 17.88%, and the percentage of zero drought condition will be increased and become 61.58%. In 2016, the extreme drought condition is decrease and become 4.09%, severe drought condition is also decrease and become 3.42%, moderate drought condition is decreased and become 8.1%, mild drought condition decrease and become 14.6%, and the percentage of zero drought condition will increase and become 69.82%. In 2017, the extreme drought again gets his height and become 5.44%, severe drought condition is increase and become 5.36%, moderate drought condition is also increase and become 9.71%, mild drought condition is increased and become 15.09%, and the percentage of zero drought condition will decrease and become 64.43%. In 2018, the extreme drought condition is increased and become 6.78%, severe drought condition is also increase and become 5.54%, moderate drought condition is again increase and become 10.36%, mild drought condition is increased and become 15.78%, and the percentage of zero drought condition will decrease and become 61.53%.

Fig. 3 shows the drought condition variation 2014-2018

Journal of Positive School Psychology
2023, Vol. 7, Issue 2
Pp 89-103

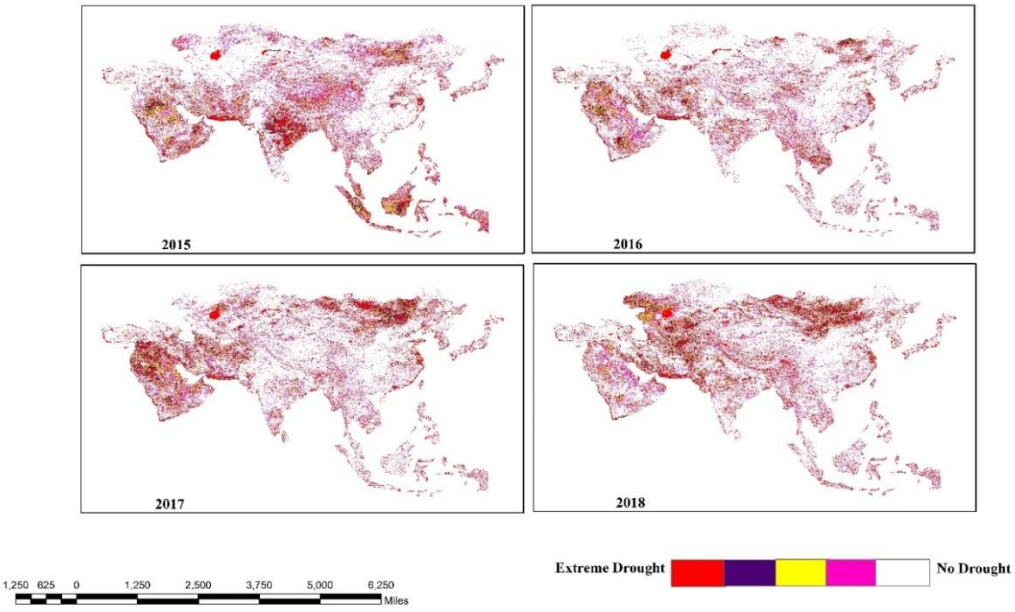

Fig. 4 shows the drought condition variation 2019-2022.

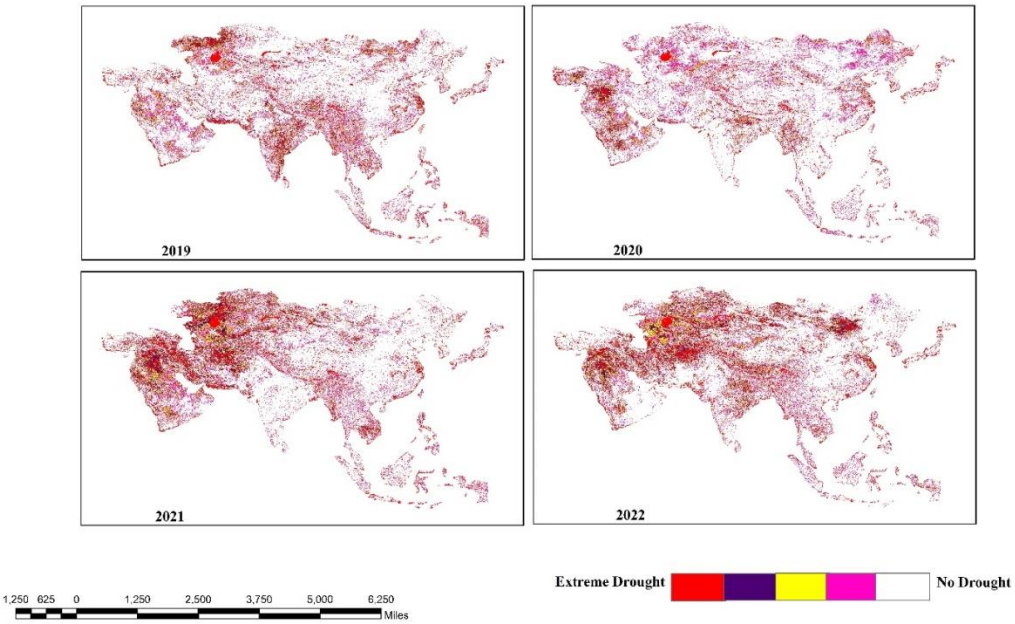

Fig. 4 shows the intensity of drought conditions in the different area of Asia like southern, northern, south-west, south-east, and central Asian regions. In 2016, the extreme drought condition is decreased and become 5.97%, severe drought condition is also decrease and become 3.90%, moderate drought condition is decrease and become 8.86%, mild drought condition is also decrease and become 15.27%, and the percentage of zero drought condition will be increased and become 66%. In 2020, the extreme drought condition is decrease and become 4.96%, severe drought condition is also decrease and become 2.42%, moderate drought condition is decreased and become 6.87%, mild drought condition increase and become 15.55%, and the percentage of zero drought condition will increase and become 70.20%. In 2021, the extreme drought again gets his height and become 8.01%, severe drought condition is increase and become 6.50%, moderate drought condition is also

increase and become 10.05%, mild drought condition is decreased and become 14.24%, and the percentage of zero drought condition will decrease and become 61.19%. In 2022, the extreme drought condition is increased and become 8.45%, severe drought condition is also increase and become 6.77%, moderate drought condition is again increase and become 10.8%, mild drought condition is decreased and become 14.03%, and the percentage of zero drought condition will decrease and become 59.95%.

Table 3 shows the drought condition variation 2011-2022 area in percentage.

Year	Extreme Drought Percentage %	Severe Drought Percentage %	Moderate Drought Percentage %	Mild Drought Percentage %	No Drought Percentage %
2011	2.008153	3.964623	12.472915	23.200305	58.354003
2012	3.110978	5.556492	12.93987	20.342891	58.049769
2013	4.221433	4.151751	11.179801	19.970702	60.476313
2014	3.995523	3.906112	10.80778	19.760136	61.530449
2015	4.893937	4.944608	10.700621	17.880178	61.580656
2016	4.091679	3.415592	8.097235	14.574021	69.821472
2017	5.44027	5.360892	9.711067	15.058638	64.429133
2018	6.778575	5.545911	10.366456	15.784047	61.525011
2019	5.965905	3.901685	8.864083	15.270806	65.997521
2020	4.957592	2.426671	6.867649	15.546797	70.201292
2021	8.013557	6.502626	10.045696	14.243944	61.194176
2022	8.452731	6.768879	10.797832	14.030976	59.949582

Authors own calculations

Empirical Results by using OLS method

This study applied Ordinary Least Square (OLS) method to examine the short run empirical relationship between the variables. The current study drawn its data from Food and Agriculture organization of United Nations (FAO) during 2011-2022. The method of OLS model for measuring the impact of severe drought on agriculture value added share of GDP in Asia is explained as

$$Yt = \beta 0 + \beta 1 Xt + \mu t \quad \ldots\ldots\ldots\ldots (10)$$ (Mahmood, Arshad, Kächele, Ullah, & Müller, 2020)

In the above empirical relationship, the study has

Yt = Agriculture value added share of GDP

Xt = Severe Drought

The estimated equation of this model is explained as:

$$Yt = 7.72 - 0.09\ Xt$$

The relationship between severe drought and agriculture value added share of GDP is negative. The impact of severe drought on agriculture value added share of GDP statistically significant at 10% level of significance.

This result implying that a 1 percent increase in severe droughts decrease the agriculture value added share of GDP by 0.09 percent.

The OLS model for measuring the impact of severe drought on agriculture value added share of GDP in Asia is explained as

$$Yt = \beta 0 + \beta 1Xt + \mu t \quad (11)$$

(Mahmood et al., 2020)

In the above-mentioned empirical relationship, this study has

Yt = Agriculture value added share of GDP

Xt = Extreme Drought

The estimated equation of this model is explained as:

$$Yt = 7.61 - 0.06\ Xt$$

Similarly, the negative and significant relation is observed between extreme drought and agriculture value added share of GDP at 10% level of significance. It means 1 percent increase in extreme drought brings 0.06 percent decline in agriculture value added share of GDP.

The equation for OLS model to measure the impact of extreme drought on food insecurity in Asia is explained as

$$Yt = \beta 0 + \beta 1Xt + \mu t \quad (12)$$ (Mahmood et al., 2020)

In the above empirical relationship, the current research has

Yt = Food insecurity

Xt = Extreme Drought

The estimated equation of this model is explained as:

$$Yt = 3.91 + 0.70\ Xt$$

This study also examined the impact of extreme drought on food insecurity in Asia by employing Ordinary Least Square method during 2014-2022. The data have been collected from FAOSTAT (2022) to measure the empirical relationship between the selected variables. The findings of the study show that extreme drought had a significant positive impact on food insecurity during 2014-2022. The results illustrate that a 1% increase in extreme drought will change .70% the food insecurity in Asia.

5. Conclusion

Agricultural drought is the slowest among all the natural hazards which develops, flourishes and spreads imperceptibly and turns green vegetated lands into barren ruin unnoticeably. In this research study remote sensing data for the agricultural drought was acquired from the United State Geological Survey website. The imagery of Landsat 7 and Landsat 8 for the years 2011-2022 were obtained and NDVI, VCI, LST, TCI and VHI analysis were performed. the drought severity was calculated in percentage on year basis which reveal that in 2011, the extreme drought condition was 2.01%, severe drought condition is 3.96%, moderate drought condition was 12.47%, mild drought condition was 23.20%, and 58.4% had zero drought condition. After a decade, the situation worsened, and the results show that the agricultural drought prevailed over a huge and vast area. In 2022, the extreme drought condition increased and became 8.45%, severe drought condition also increased and reached to 6.77%, moderate drought condition soared to 10.8%, mild drought condition decreased and became 14.03%, and the percentage of zero drought condition also saw a decline and settled at 59.95%. The findings of OLS method illustrate that severe drought had a significant negative impact on agriculture value added share of GDP. The negative and significant relation is observed between extreme drought and agriculture value added share of GDP. Further, the extreme drought had a significant positive impact on food insecurity during the selected time span. All this show that the agricultural drought is swallowing the vegetated parts of the Asian land rapidly in an unperceivable and subtle way. The south-west Asia faces more drought conditions as compared to Central Asia. The equatorial region of Asia faces moderate and mild drought conditions.

References

1. Alves, E. D. L. (2016). Seasonal and spatial variation of surface urban heat island intensity in a small urban agglomerate in Brazil. Climate, 4(4), 61.
2. Andersson, L., Wilk, J., Graham, L. P., Wikner, J., Mokwatlo, S., & Petja, B. (2020). Local early warning systems for drought–Could they add value to nationally disseminated seasonal climate forecasts? Weather and Climate Extremes, 28, 100241.
3. Araneda-Cabrera, R. J., Bermúdez, M., & Puertas, J. (2021). Assessment of the performance of drought indices for explaining crop yield variability at the national scale: Methodological framework and application to Mozambique. Agricultural Water Management, 246, 106692.
4. Bajgain, R., Xiao, X., Basara, J., Wagle, P., Zhou, Y., Zhang, Y., & Mahan, H. (2017). Assessing agricultural drought in summer over Oklahoma Mesonet sites using the water-related vegetation index from MODIS. International journal of biometeorology, 61, 377-390.
5. Bajgain, R., Xiao, X., Wagle, P., Basara, J., & Zhou, Y. (2015). Sensitivity analysis of vegetation indices to drought over two tallgrass prairie sites. ISPRS Journal of Photogrammetry and Remote Sensing, 108, 151-160.
6. Bayissa, Y., Tadesse, T., & Demisse, G. (2019). Building a high-resolution vegetation outlook model to monitor agricultural drought for the Upper Blue Nile Basin, Ethiopia. Remote Sensing, 11(4), 371.
7. Bento, V. A., Gouveia, C. M., DaCamara, C. C., Libonati, R., & Trigo, I. F. (2020). The roles of NDVI and Land Surface Temperature when using the Vegetation Health Index over dry regions. Global and Planetary Change, 190, 103198.
8. Berger, A., Ettlin, G., Quincke, C., & Rodríguez-Bocca, P. (2019). Predicting the Normalized Difference Vegetation Index (NDVI) by training a crop growth model with historical data. Computers and Electronics in Agriculture, 161, 305-311.
9. Bezdan, J., Bezdan, A., Blagojević, B., Mesaroš, M., Pejić, B., Vranešević, M., . . . Nikolić-Đorić, E. (2019). SPEI-based approach to agricultural drought monitoring in Vojvodina region. Water, 11(7), 1481.
10. Bustos, E., & Meza, F. J. (2015). A method to estimate maximum and minimum air temperature using MODIS surface temperature and vegetation data: application to the Maipo Basin, Chile. Theoretical and Applied Climatology, 120, 211-226.
11. Chandrasekara, S. S., Kwon, H.-H., Vithanage, M., Obeysekera, J., & Kim, T.-W. (2021). Drought in South Asia: A review of drought assessment and prediction in South Asian countries. Atmosphere, 12(3), 369.
12. Chen, S., Zhong, W., Pan, S., Xie, Q., & Kim, T.-W. (2020). Comprehensive drought assessment using a modified composite drought index: A case study in Hubei Province, China. Water, 12(2), 462.
13. Cheng, C.-H., Nnadi, F., & Liou, Y.-A. (2015). A regional land use drought index for Florida. Remote Sensing, 7(12), 17149-17167.
14. Clark, M. L., & Roberts, D. A. (2012). Species-level differences in hyperspectral metrics among tropical rainforest trees as determined by a tree-based classifier. Remote Sensing, 4(6), 1820-1855.
15. Das, A. C., Noguchi, R., & Ahamed, T. (2021). An assessment of drought stress in tea estates using optical and thermal remote sensing. Remote Sensing, 13(14), 2730.

16. Dikshit, A., Pradhan, B., & Huete, A. (2021). An improved SPEI drought forecasting approach using the long short-term memory neural network. Journal of environmental management, 283, 111979.
17. Dutta, D., Kundu, A., Patel, N., Saha, S., & Siddiqui, A. (2015). Assessment of agricultural drought in Rajasthan (India) using remote sensing derived Vegetation Condition Index (VCI) and Standardized Precipitation Index (SPI). The Egyptian Journal of Remote Sensing and Space Science, 18(1), 53-63.
18. Fang, H., Liang, S., & Hoogenboom, G. (2011). Integration of MODIS LAI and vegetation index products with the CSM–CERES–Maize model for corn yield estimation. International journal of remote sensing, 32(4), 1039-1065.
19. Finnessey, T., Hayes, M., Lukas, J., & Svoboda, M. (2016). Using climate information for drought planning. Climate Research, 70(2-3), 251-263.
20. Fu, B., & Burgher, I. (2015). Riparian vegetation NDVI dynamics and its relationship with climate, surface water and groundwater. Journal of Arid Environments, 113, 59-68.
21. Gao, B.-C., & Li, R.-R. (2000). Quantitative improvement in the estimates of NDVI values from remotely sensed data by correcting thin cirrus scattering effects. Remote Sensing of environment, 74(3), 494-502.
22. Gao, X., Xu, Y., Zhao, Z., Pal, J., & Giorgi, F. (2006). On the role of resolution and topography in the simulation of East Asia precipitation. Theoretical and Applied Climatology, 86, 173-185.
23. Gao, Y., Gao, M., Damdinsuren, B., & Dorjsuren, M. (2021). Early drought warning based on chlorophyll fluorescence and normalized difference vegetation index in Xilingol League of China. Journal of Applied Remote Sensing, 15(3), 032006-032006.
24. Gebrehiwot, T., Van der Veen, A., & Maathuis, B. (2011). Spatial and temporal assessment of drought in the Northern highlands of Ethiopia. International Journal of Applied Earth Observation and Geoinformation, 13(3), 309-321.
25. Gebrehiwot, T., Van der Veen, A., & Maathuis, B. (2016). Governing agricultural drought: Monitoring using the vegetation condition index. Ethiopian journal of environmental studies and management, 9(3), 354-371.
26. Ghazaryan, G., Dubovyk, O., Graw, V., Kussul, N., & Schellberg, J. (2020). Local-scale agricultural drought monitoring with satellite-based multi-sensor time-series. GIScience & Remote Sensing, 57(5), 704-718.
27. Groten, S. (1993). NDVI—crop monitoring and early yield assessment of Burkina Faso. TitleREMOTE SENSING, 14(8), 1495-1515.
28. Guo, J., Ren, H., Zheng, Y., Lu, S., & Dong, J. (2020). Evaluation of land surface temperature retrieval from Landsat 8/TIRS images before and after stray light correction using the SURFRAD dataset. Remote Sensing, 12(6), 1023.
29. Han, H., Bai, J., Yan, J., Yang, H., & Ma, G. (2021). A combined drought monitoring index based on multi-sensor remote sensing data and machine learning. Geocarto International, 36(10), 1161-1177.
30. Hanade Houmma, I., El Mansouri, L., Gadal, S., Mamane Barkawi, M. B., & Hadria, R. (2022). Prospective analysis of spatial heterogeneity influence on the concordance of remote sensing drought indices: a case of semi-arid agrosystems in Morocco (Moulouya and Tensift watersheds). Geocarto International, 37(27), 14899-14924.
31. Hara, P., Piekutowska, M., & Niedbała, G. (2021). Selection of independent variables for crop yield prediction using artificial neural network models with remote sensing data. Land, 10(6), 609.
32. How Jin Aik, D., Ismail, M. H., & Muharam, F. M. (2020). Land use/land cover changes and the relationship with land surface temperature using Landsat and MODIS imageries in Cameron Highlands, Malaysia. Land, 9(10), 372.
33. Jiménez-Donaire, M. d. P., Giráldez, J. V., & Vanwalleghem, T. (2020). Evaluation of drought stress in cereal through probabilistic modelling of soil moisture dynamics. Water, 12(9), 2592.
34. Kogan, F. (2002). World droughts in the new millennium from AVHRR-based vegetation health indices. Eos, Transactions American Geophysical Union, 83(48), 557-563.
35. Kogan, F. N. (1995). Application of vegetation index and brightness temperature for drought detection. Advances in space research, 15(11), 91-100.
36. Kulkarni, S. S., Wardlow, B. D., Bayissa, Y. A., Tadesse, T., Svoboda, M. D., & Gedam, S. S. (2020). Developing a remote sensing-based combined drought indicator approach for agricultural drought monitoring over Marathwada, India. Remote Sensing, 12(13), 2091.
37. Liu, X., Zhu, X., Pan, Y., Bai, J., & Li, S. (2018). Performance of different drought indices for agriculture drought in the North China Plain. Journal of Arid Land, 10, 507-516.
38. Liu, X., Zhu, X., Zhang, Q., Yang, T., Pan, Y., & Sun, P. (2020). A remote sensing and artificial neural network-based integrated agricultural drought index: Index development and applications. Catena, 186, 104394.
39. Lott, N., & Ross, T. (2006). 1.2 Tracking and evaluating US billion dollar weather disasters, 1980–2005.

Retrieved on March.
40. Mahmood, N., Arshad, M., Kächele, H., Ullah, A., & Müller, K. (2020). Economic efficiency of rainfed wheat farmers under changing climate: Evidence from Pakistan. Environmental Science and Pollution Research, 27, 34453-34467.
41. Mishra, A. K., & Singh, V. P. (2010). A review of drought concepts. Journal of hydrology, 391(1-2), 202-216.
42. Mullapudi, A., Vibhute, A. D., Mali, S., & Patil, C. H. (2023). A review of agricultural drought assessment with remote sensing data: methods, issues, challenges and opportunities. Applied Geomatics, 15(1), 1-13.
43. Nam, W.-H., Choi, J.-Y., Yoo, S.-H., & Engel, B. (2012). A real-time online drought broadcast system for monitoring soil moisture index. KSCE Journal of Civil Engineering, 16, 357-365.
44. Nam, W.-H., Hayes, M. J., Svoboda, M. D., Tadesse, T., & Wilhite, D. A. (2015). Drought hazard assessment in the context of climate change for South Korea. Agricultural Water Management, 160, 106-117.
45. Nam, W.-H., Tadesse, T., Wardlow, B. D., Hayes, M. J., Svoboda, M. D., Hong, E.-M., . . . Jang, M.-W. (2018). Developing the vegetation drought response index for South Korea (VegDRI-SKorea) to assess the vegetation condition during drought events. International journal of remote sensing, 39(5), 1548-1574.
46. Naumann, G., Dutra, E., Barbosa, P., Pappenberger, F., Wetterhall, F., & Vogt, J. (2014). Comparison of drought indicators derived from multiple data sets over Africa. Hydrology and Earth System Sciences, 18(5), 1625-1640.
47. Otkin, J. A., Anderson, M. C., Hain, C., & Svoboda, M. (2014). Examining the relationship between drought development and rapid changes in the evaporative stress index. Journal of Hydrometeorology, 15(3), 938-956.
48. Putnam, A. E., Putnam, D. E., Andreu-Hayles, L., Cook, E. R., Palmer, J. G., Clark, E. H., . . . Boyle, D. P. (2016). Little Ice Age wetting of interior Asian deserts and the rise of the Mongol Empire. Quaternary Science Reviews, 131, 33-50.
49. Quarmby, N., Milnes, M., Hindle, T., & Silleos, N. (1993). The use of multi-temporal NDVI measurements from AVHRR data for crop yield estimation and prediction. International journal of remote sensing, 14(2), 199-210.
50. Seiler, R., Kogan, F., & Sullivan, J. (1998). AVHRR-based vegetation and temperature condition indices for drought detection in Argentina. Advances in space research, 21(3), 481-484.
51. Sevanto, S. (2018). Drought impacts on phloem transport. Current Opinion in Plant Biology, 43, 76-81.
52. Sobrino, J. A., Jiménez-Muñoz, J. C., & Paolini, L. (2004). Land surface temperature retrieval from LANDSAT TM 5. Remote Sensing of environment, 90(4), 434-440.
53. Song, Y., Wang, J., Ge, Y., & Xu, C. (2020). An optimal parameters-based geographical detector model enhances geographic characteristics of explanatory variables for spatial heterogeneity analysis: Cases with different types of spatial data. GIScience & Remote Sensing, 57(5), 593-610.
54. Svoboda, M. (2000). An introduction to the drought monitor.
55. Tadesse, T., Brown, J. F., & Hayes, M. J. (2005). A new approach for predicting drought-related vegetation stress: Integrating satellite, climate, and biophysical data over the US central plains. ISPRS Journal of Photogrammetry and Remote Sensing, 59(4), 244-253.
56. Tomar, V., Kumar, P., Rani, M., Gupta, G., & Singh, J. (2013). A satellite-based biodiversity dynamics capability in tropical forest. Electron. J. Geotech. Eng, 18, 1171-1180.
57. Vicente-Serrano, S. M., Beguería, S., & López-Moreno, J. I. (2010). A multiscalar drought index sensitive to global warming: the standardized precipitation evapotranspiration index. Journal of climate, 23(7), 1696-1718.
58. Wang, P. (2004). Cenozoic deformation and the history of sea-land interactions in Asia. Geophysical Monograph Series, 149, 1-22.
59. West, H., Quinn, N., & Horswell, M. (2019). Remote sensing for drought monitoring & impact assessment: Progress, past challenges and future opportunities. Remote Sensing of environment, 232, 111291.
60. Wildemeersch, J. C., Garba, M., Sabiou, M., Fatondji, D., & Cornelis, W. M. (2015). Agricultural drought trends and mitigation in Tillaberí, Niger. Soil science and plant nutrition, 61(3), 414-425.
61. Wilhite, D. A., & Glantz, M. H. (1985). Understanding: the drought phenomenon: the role of definitions. Water international, 10(3), 111-120.
62. Yang, Y., Guan, H., Batelaan, O., McVicar, T. R., Long, D., Piao, S., . . . Simmons, C. T. (2016). Contrasting responses of water use efficiency to drought across global terrestrial ecosystems. Scientific Reports, 6(1), 23284.
63. Zhang, L., Jiao, W., Zhang, H., Huang, C., & Tong, Q. (2017). Studying drought phenomena in the Continental United States in 2011 and 2012 using various drought indices. Remote Sensing of

environment, 190, 96-106.
64. Zhong, S., Di, L., Sun, Z., Xu, Z., & Guo, L. (2019). Investigating the long-term spatial and temporal characteristics of vegetative drought in the contiguous United States. IEEE Journal of Selected Topics in Applied Earth Observations and Remote Sensing, 12(3), 836-848.
65. Zhou, Y., Xiao, X., Zhang, G., Wagle, P., Bajgain, R., Dong, J., . . . Hain, C. (2017). Quantifying agricultural drought in tallgrass prairie region in the US Southern Great Plains through analysis of a water-related vegetation index from MODIS images. Agricultural and Forest Meteorology, 246, 111-122.